Automatic Advance Angle Control Algorithm Using Anti-Windup Feedback Voltage of PI Current Controller for Wide Range Speed Operation of BLDCM

Min-Hyo Lee
H&A Control R&D Lab.
LG Electronics
Changwon, Korea
Minhyo.lee@lge.com

Ho-Jin Kim
Future Transport Machinery Center
Busan Techno-Park
Busan, Korea
khj@btp.or.kr

Hyeong-Jin Kim, Jang-Mok Kim
Dept. of Electrical Engineering
Pusan National University
Busan, Korea
{hyeongjin628, jmok}@pusan.ac.kr

***Abstract*— This paper proposes the automatic advance angle control algorithm that does not use the lookup table and the voltage equation of BLDCM. An advance angle control can obtain the relatively large voltage margin by pulling the conduction angle of the phase current against the back-EMF to expand the speed range of the motor. The conventional paper using the lookup table is difficult to control the speed and produce the torque accurately, because the error of the advance angle occurs when the electrical parameters of the motor are varied by the change of the temperature and the operating conditions. Since the anti-windup output signal of the PI current controller is used as the input signal of the proposed advance angle control algorithm, the proposed algorithm is not only robust against the electrical constant changes of the motor but also excellent in the transient state of the various operating conditions. The proposed algorithm has the additional features that the implementation is simple and the efficient operation is possible in the high speed region. The usefulness of the proposed algorithm is verified through simulation results.**

Keywords—Advance angle; BLDCM; Anti-Windup controller;

I. INTRODUCTION

Three-Phase BLDCM(Brushless DC Motor) is used in a variety of industry applications due to simple structure, high efficiency and low-maintenance. BLDCM with the trapezoidal back-EMF is controlled by the square wave current and has a larger torque and a higher power density than PMSM (Permanent Magnet Synchronous Motor) with the sinusoidal back-EMF and the sine wave current [1], [2].

In the high speed region of the motor, the voltage shortage occurs due to the large back-EMF and the phase current is delayed by the increase of the phase reactance as shown in Fig. 1 (a). PMSM(Permanent Magnet Synchronous Motor) applies the field weakening control algorithm to control the *d*-axis current for these problems, but BLDCM with the trapezoidal back-EMF cannot apply the algorithm because the *d-q* conversion for vector control is not used in BLDCM [3], [4]. Therefore, BLDCM uses the advance angle control algorithm that controls the phase current by angle of lead than back-EMF as shown in Fig. 1 (b) [5].

The conventional advance angle control algorithm controls the advance angle through the lookup table of the advance angle to the speed [2], [6]. The algorithm has disadvantages that the rated conditions of the motor are essential and further experiments are required to make the lookup table. Also, if the operating point is changed by the change of the temperature, the error of the advance angle occurs and the response characteristic deteriorates in the high speed region.

This paper proposes the algorithm that automatically calculates the appropriate advance angle regardless of the parameter changes or the operating conditions by using the anti-windup output of the PI current controller, and obtains the voltage margin to expand the speed range of BLDCM. And the usefulness of the proposed algorithm is verified by simulation results.

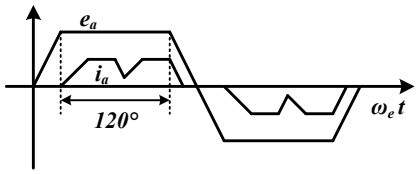

(a) Without advance angel control algorithm

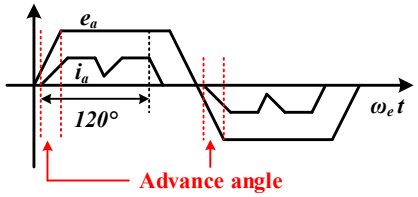

(b) With advance angle control algorithm

Fig. 1. Back-EMF and phase current of BLDCM in high speed region

II. PROPOSED ADVANCE ANGLE CONTROL ALGORITHM

A. Analysis of Voltage Margin in BLDCM

Fig. 2 (a) shows the phase voltage and the back-EMF waveforms of ideal three-phase BLDCM. The voltage equation of BLDCM is shown in Eq. (1). Where V_{DC} is DC link voltage, R_s is phase resistance, L_s is phase inductance, and i_a, i_b are a-, b-phase currents, and E_a, E_b are a-, b-phase back-EMF. When BLDCM is controlled by the two-phase excitation method, Eq. (1) can be expressed as Eq. (2) since i_b, E_b are equal to $-i_a$, $-E_a$ respectively.

$$V_{DC} = R_s i_a + L_s \frac{di_a}{dt} + E_a - (R_s i_b + L_s \frac{di_b}{dt} + E_b) \quad (1)$$

$$0.5V_{DC} - E_a = R_s i_a + L_S \frac{di_a}{dt} \quad (2)$$

As shown in Eq. (2), the phase current of BLDCM is determined by the difference between the applied voltage and the back-EMF. According to C. C. Chan's paper [2], it is known that the voltage drop component of the inductance can suppress the increase of the back-EMF. Therefore, Eq. (2) can be expressed by Eq. (3) and is equal to the voltage margin when the advance angle control is not applied as shown in Fig. 2. (a). Where V_{eff} is the voltage margin, E is the magnitude of the back-EMF in the region where the back-EMF is constant. As the speed increases, the back-EMF increases and the voltage margin becomes insufficient above the rated speed.

$$V_{eff} = 0.5V_{DC} - E - R_s i_a = L\frac{di_a}{dt} \quad (3)$$

However, the phase voltage is applied even in the region where the back-EMF is not constant when the advance angle control is applied as shown in Fig. 2 (b). The additional voltage margin is equal to the triangle of the area in Fig. 2 (b), and can be expressed as the rightmost term of Eq. (4). In Fig. 2 (b), θ_0 is the advance angle of the phase current. Since the voltage margin is increased by pulling the angle of the current against in left direction of Fig. 2 (b), the high-speed control is possible with the constant DC link voltage.

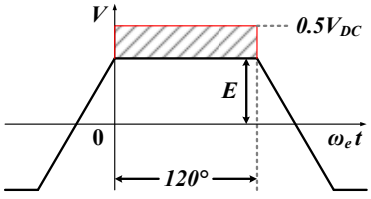

(a) Without advance angle control algorithm

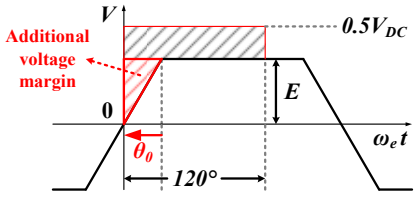

(b) With advance angle control algorithm

Fig. 2. Waveforms of phase voltage and back-EMF

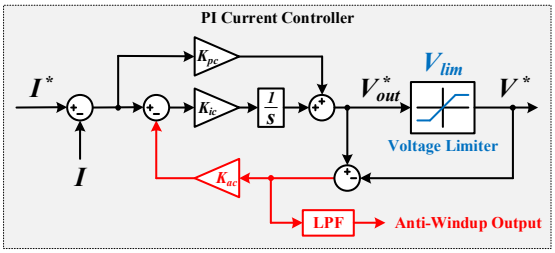

Fig. 3. Block diagram of PI current controller with anti-windup controller

$$V_{eff} = (0.5V_{DC} - E - R_s i_a) + \frac{9E}{2\pi^2}\theta_0^2 \quad (4)$$

B. Anti-Windup Output of PI Current Controller for the Proposed Algorithm

The block diagram of the PI current controller with the anti-windup controller is shown in Fig. 3. The transfer function of the current controller is shown in Eq. (5). The anti-windup output signal is generated when the voltage reference, which is the output of the PI current controller, is greater than the limit voltage, and is the same as the rightmost term of Eq. (5) [7].

$$I = \frac{K_{pc}s + K_{ic}}{L_s s^2 + (R_s + K_{pc})s + K_{ic}}[I^* - \frac{s + K_{ac}K_{ic}}{K_{pc}s + K_{ic}}(V^*_{out} - V^*)] \quad (5)$$

Fig. 4 (a) shows the waveforms of the anti-windup output at the low speed and light load conditions, and it has pulse forms in the commutation period of BLDCM due to the high bandwidth of the PI current controller. But, the pulse forms are removed by the LPF(Low Pass Filter) and becomes zero. Fig. 4 (b) shows the waveforms of the anti-windup output signal at the high speed and heavy load conditions, the signal is converges to a constant value with the noise removed by the LPF. This value is directly related to the back-EMF of BLDCM.

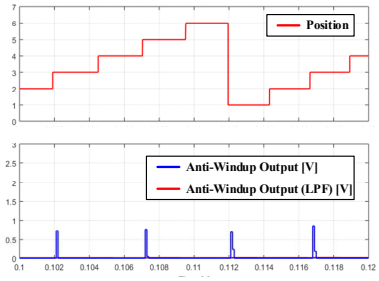

(a) Low speed region

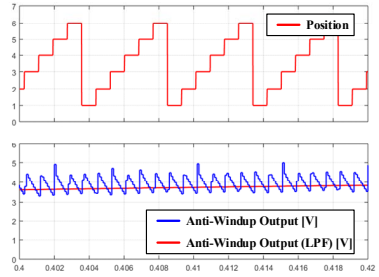

(b) High speed region

Fig. 4. Rotor position, anti-windup output and LPF output

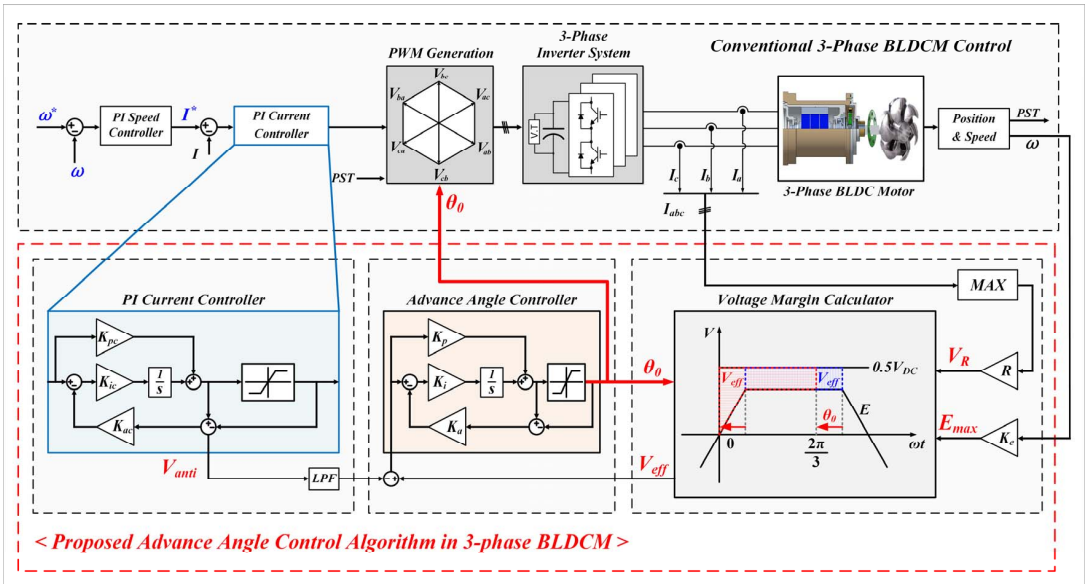

Fig. 5 Block diagram of proposed advance angle control algorithm

The proposed automatic advance angle control algorithm calculates the advance angle using the anti-windup output of PI current controller and the voltage margin. As described above, the anti-windup output is generated when the voltage is insufficient. The noise included in the anti-windup output is removed through the LPF and used as the input signal to the advance angle controller. The input signal is compared with the voltage margin of the system, and the advance angle is output through the PI controller. The block diagram of the proposed advance angle control algorithm is shown in Fig. 5.

III. Simulation Results

The validity of the proposed automatic advance angle control algorithm is verified by the simulation in the BLDCM speed control system. The parameters used in the simulation are shown in Table 1. The speed reference 2,500 RPM, which is above the rated speed, and the load increases from 0.1 Nm to 0.3 Nm when the speed response reaches the steady state.

TABLE I. Parameters of BLDCM

DC Link Voltage	24 [V]	Poles	10
Rated Torque	0.4 [Nm]	Stator Resistance	0.5 [Ω]
Rated Speed	2,000 [RPM]	Stator Inductance	565 [uH]
Rated Power	100 [W]	Back-EMF Constant	0.04108 [V/rad/s]

Fig. 6 shows the speed and current response waveforms when an advance angle control algorithm is not used. Current control is not possible due to the voltage shortage caused by the increase in speed. and therefore the speed response also fails to reach the speed reference when the load increases.

Fig. 7 shows the speed, current response and the applied advance angle waveforms when using the conventional advance angle control algorithm with the look-up table defined in the rated condition is applied. Speed control is possible by the applied advance angle, but the speed response is delayed by the voltage shortage when the speed increases. In addition, since the load condition of 0.1 Nm is not considered in the look-up table, the excessive advance angle is applied and the current ripple becomes large.

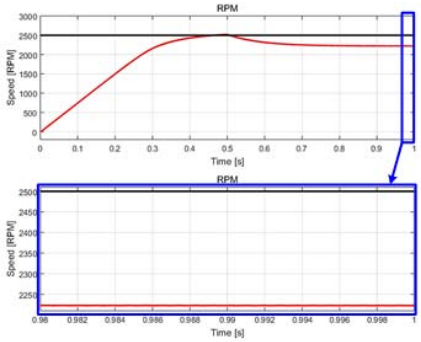

(a) Speed response

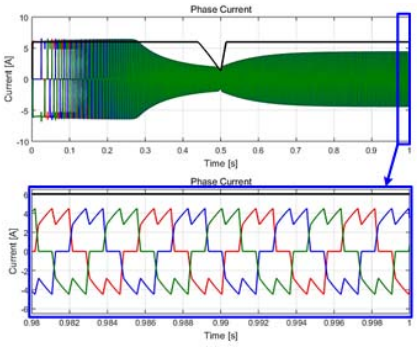

(b) Current response

Fig. 6. Waveforms of high speed control without algorithm

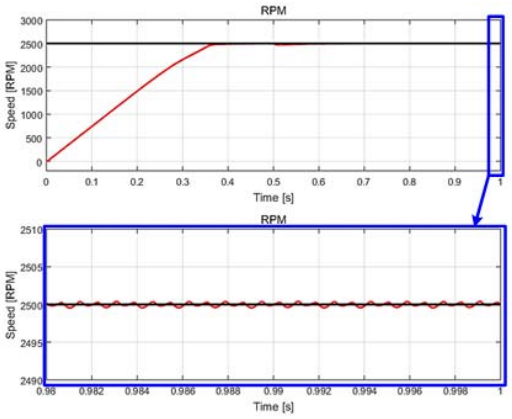

(a) Speed response

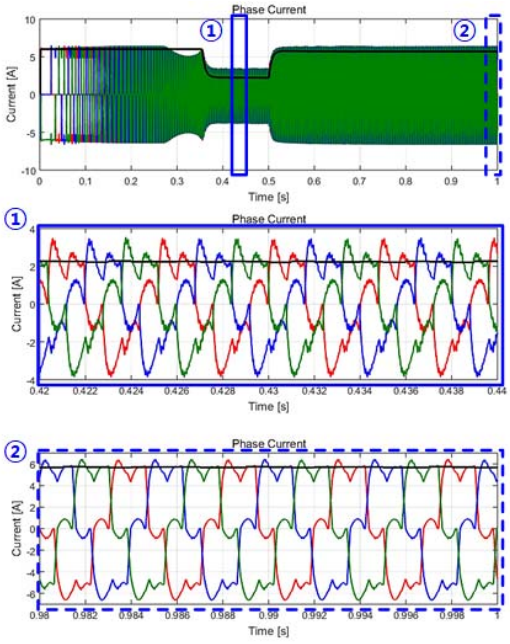

(b) Current response

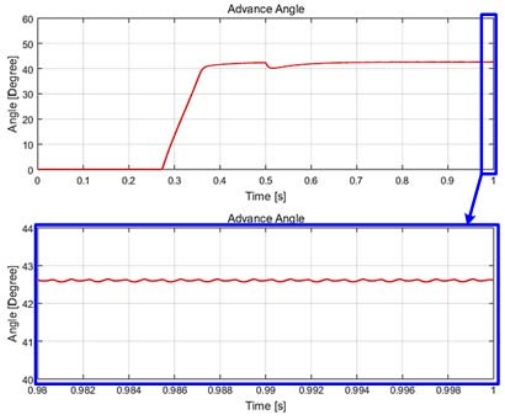

(c) Advance angle

Fig. 7. Waveforms of high speed control with conventional algorithm

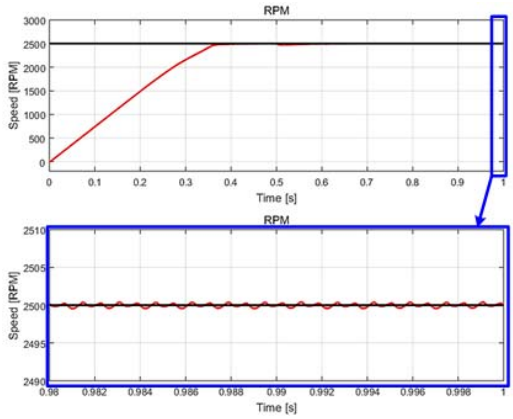

(a) Speed response

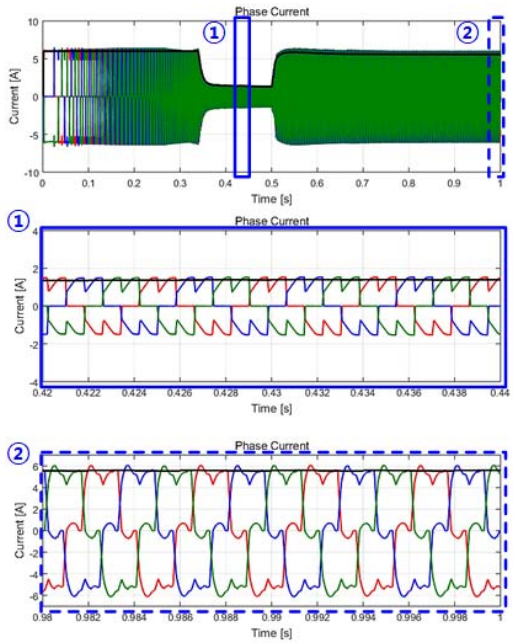

(b) Current response

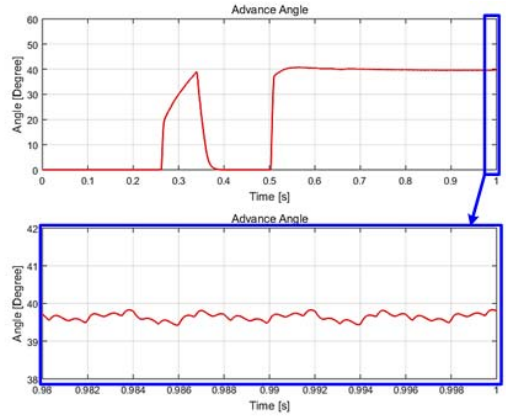

(c) Advance angle

Fig. 8. Waveforms of high speed control with proposed algorithm

Fig. 8 shows the speed, current response and the applied advance angle waveforms when using the proposed automatic advance angle control algorithm. Since the proposed algorithm uses the anti-windup output of the PI current controller for the advance angle control, the speed and current conditions of the system are considered simultaneously. Therefore, there is no region where the voltage shortage or the excessive advance angle is applied.

The effect of the parameter changes that occur when the temperature condition changes in the system using the proposed algorithm is shown in Fig. 9, 10. The advance angle is appropriately controlled and the high-speed operation is possible regardless of the parameter changes depending on the temperature.

The simulation waveforms for the four-quadrant operation of the system using the proposed algorithm is as shown in Fig. 11. When the speed reference changes from 2500 RPM to -2500 RPM, the advance angle also changes according to the operating conditions of the system and allows the four-quadrant operation.

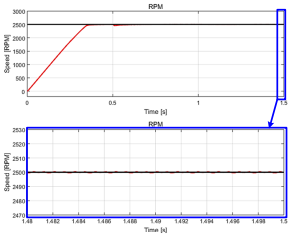

(a) Speed response

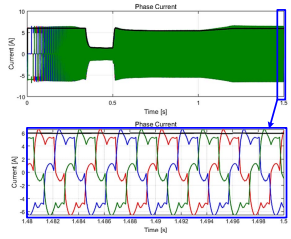

(b) Current response

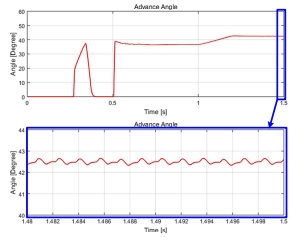

(c) Advance angle

Fig. 9. Waveforms of high speed control with proposed algorithm at -10 □

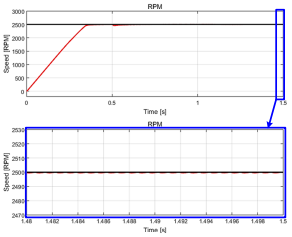

(a) Speed response

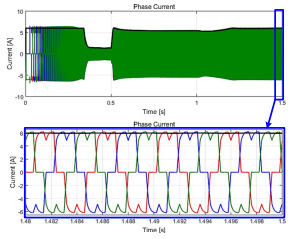

(b) Current response

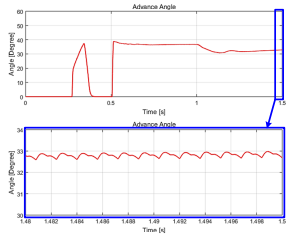

(c) Advance angle

Fig. 10. Waveforms of high speed control with proposed algorithm at 120 □

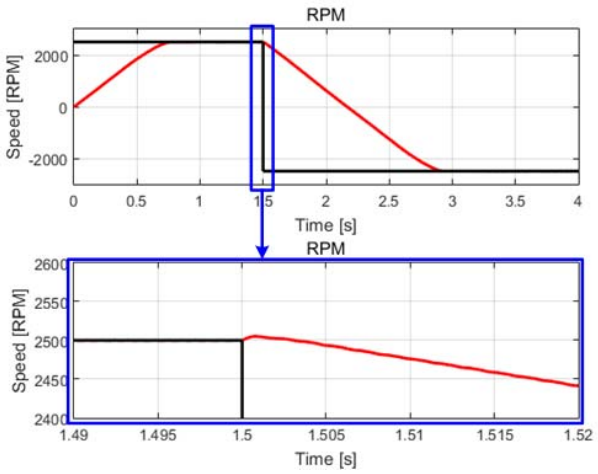

(a) Speed response

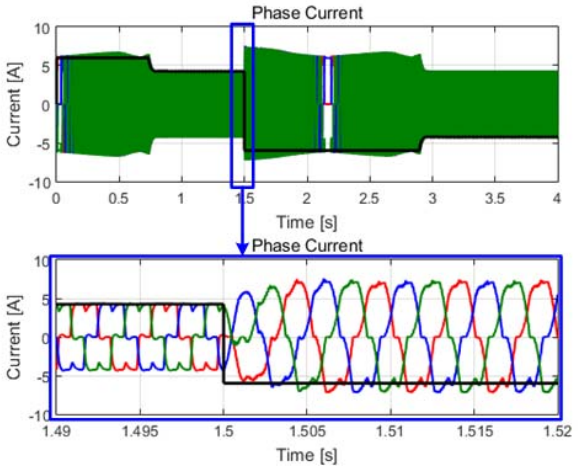

(b) Current response

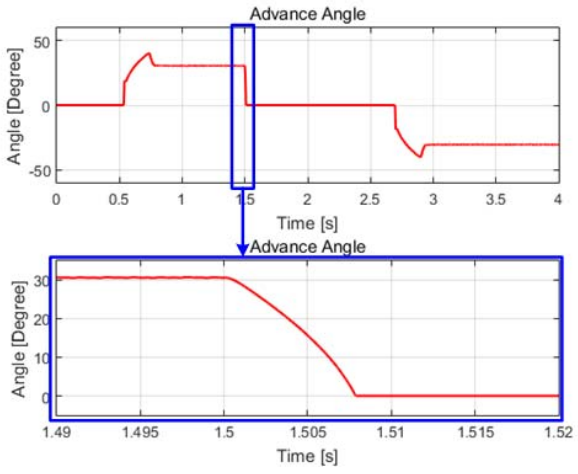

(c) Advance angle

Fig. 10. Waveforms of four-quadrant operation with proposed algorithm

IV. CONCLUSION

The proposed automatic advance angle control algorithm controlled automatically the advance angle according to the anti-windup output and the voltage margin for the wide range speed operation. As shown in the simulation results, the proposed algorithm was robust against the parameter errors and four-quadrant operation was possible. Also, it had additional features that the implementation is simple and the performance of the high speed control is excellent. The usefulness of the proposed algorithm was verified through simulation results.

ACKNOWLEDGMENT

This research was supported by the Ministry of Trade, Industry & Energy(MOTIE), Korea Institute for Advancement of Technology(KIAT) through the Encouragement Program for The Industries of Economic Cooperation Region

REFERENCES

[1] Gilliam, J. E. "Brushless Permanent-Magnet and Reluctance Motor Drives." Power Engineering Journal 4.1 (1990): 20-20.

[2] Chan, C. C., Jiang, J. Z., Xia, W., & Chan, K. T. (1995). Novel wide range speed control of permanent magnet brushless motor drives. IEEE transactions on power electronics, 10(5), 539-546.

[3] Weh, H., H. Mosebach, and H. May. "Design concepts and force generation in inverter-fed synchronous machines with permanent magnet excitation." IEEE Transactions on Magnetics 20.5 (1984): 1756-1761.

[4] Bailey, J. M., J. S. Lawler, and B. Banerjee. "Five Phase Trapezoidal Back Emf PM Synchronous Machines and Drives." Proc. European Power Electron. Conference.

[5] Im, Won-Sang, et al. "Torque maximization control of 3-phase BLDC motors in the high speed region." Journal of Power Electronics 10.6 (2010): 717-723.

[6] Nguyen, BinhMinh, and Minh C. Ta. "Phase advance approach to expand the speed range of brushless DC motor." Power Electronics and Drive Systems, 2007. PEDS'07. 7th International Conference on. IEEE, 2007.

[7] Yoo, Hyun-Jae, Yu-Seok Jeong, and Seung-Ki Sul. "Anti-windup for Complex Vector Synchronous Frame PI Current Controller." The Transactions of the Korean Institute of Power Electronics 11.5 (2006): 404-408.